ORIGINAL PAPER

In-silico modeling of a novel OXA-51 from β-lactam-resistant *Acinetobacter baumannii* and its interaction with various antibiotics

Vishvanath Tiwari · Isha Nagpal · Naidu Subbarao · Rajeswari R. Moganty

Abstract *Acinetobacter baumannii*, one of the major Gram negative bacteria, causes nosocomial infections such as pneumonia, urinary tract infection, meningitis, etc. β-lactam-based antibiotics like penicillin are used conventionally to treat infections of *A. baumannii*; however, they are becoming progressively less effective as the bacterium produces diverse types of β-lactamases to inactivate the antibiotics. We have recently identified a novel β-lactamase, OXA-51 from clinical strains of *A. baumannii* from our hospital. In the present study, we generated the structure of OXA-51 using MODELLER9v7 and studied the interaction of OXA-51 with a number of β-lactams (penicillin, oxacillin, ceftazidime, aztreonam and imipenem) using two independent programs: GLIDE and GOLD. Based on the results of different binding parameters and number of hydrogen bonds, interaction of OXA-51 was found to be maximum with ceftazidime and lowest with imipenem. Further, molecular dynamics simulation results also support this fact. The lowest binding affinity of imipenem to OXA-51 indicates clearly that it is not efficiently cleaved by OXA-51, thus explaining its high potency against resistant *A. baumannii*. This finding is supported by experimental results from minimum inhibitory concentration analysis and transmission electron microscopy. It can be concluded that carbapenems (imipenem) are presently effective β-lactam antibiotics against resistant strains of *A. baumannii* harbouring OXA-51. The results presented here could be useful in designing more effective derivatives of carbapenem.

Keywords *Acinetobacter baumannii* · OXA-51 · β-lactamase · β-lactam · Antibiotic resistance · GLIDE

V. Tiwari · R. R. Moganty (✉)
Department of Biochemistry,
All India Institute of Medical Sciences,
Ansari Nagar,
New Delhi 110029, India
e-mail: rajeswari3011@hotmail.com

I. Nagpal · N. Subbarao
School of Computational and Integrative Sciences,
Jawaharlal Nehru University,
New Delhi, India

Introduction

Acinetobacter baumannii, an opportunistic pathogen, is well known to cause a wide spectrum of nosocomial infections, particularly in intensive care units of hospitals. *A. baumannii* is known to cause pneumonia, bloodstream infections, surgical site infections and urinary tract infections [1]. *A. baumannii* is found in most clinical isolates after disasters of war [2–5], and was considered as the main culprit for the death of soldiers during the Iraq war [6]. Many reports have been published worldwide regarding the outbreaks and pathology of *A. baumannii* [7–13]. Its prevalence (26%) in the All India Institute of Medical Sciences (AIIMS), New Delhi, India [14] has increased gradually, and had reached 31% by 2009 (unpublished data).

Owing to their high effectiveness, low cost, ease of delivery and minimal side effects, β-lactams are the antibiotics used most widely in treating infections caused by *A. baumannii*. β-lactam antibiotics are classified broadly into four groups; the early discovered penicillins (e.g., peniciilin and oxacillin, etc.), followed by cephalosporins (e.g., ceftazidime, etc.), monobactams (e.g., aztreonam, etc.) and carbapenems (e.g., imipenem, etc.). The prevalence of β-lactam-resistant clinical isolates that are non-susceptible to most classes of antibiotics is increasing worldwide [15, 16]. In response to their extensive use, reports from all over the world reveal that

the β-lactam resistance rate has increased from 0–2% in the 1990s to 38–71% in 2008 [17]. In the last 20 years, *A. baumannii* has demonstrated a remarkable ability to develop and share resistance to every antibiotic that has been developed. *A. baumannii* developed resistance often by quite unexpected mechanisms and much more rapidly than was originally predicted [18–23]. The continued utility of β-lactams is threatened by the expression of β-lactamase enzymes, the most pervasive mechanism against this class of antibiotics. As the name suggests, β-lactamase hydrolyzes the β-lactam ring and renders the antibiotic inactive against its original cellular targets: cell wall transpeptidases. OXA β-lactamases have emerged recently in different parts of the world [18, 19, 24, 25]. A total of eight subgroups of OXA has been identified in Gram negative bacteria; four of these have been reported in *A. baumannii* [20]. OXA-51 has been found in β-lactam-resistant strains of *A. baumannii* from India (our unpublished data). Thus, we wanted to study the interaction of different β-lactams with OXA-51 in order to understand the resistance mechanism at the structural level.

Materials and methods

Comparative modeling of OXA-51 β-lactamase

Selection of template

The amino acid sequence of OXA-51 β-lactamase of *A. baumannii* (target OXA-51) was retrieved from the sequence database of NCBI (http://www.ncbi.nlm.nih.gov) (accession no. gb: ABD47672, 274aa). To identify the templates for homology modeling of OXA-51, a BLASTP search (http://blast.ncbi.nlm.nih.gov/Blast.cgi?PAGE=Proteins) was performed against the Brookhaven Protein Data Bank with the default parameters.

MODELER9v7

The academic version of MODELER9v7 (http://:www.salilab.org/modeler), was used for 3D structure generation of OXA-51. The 3D model of OXA-51 was obtained by optimization of the molecular probability density function (pdf) such that the model as much as possible does not violate the input restraints. The residue profiles of the three-dimensional models were further checked using VERIFY3D. PROCHECK (http://nihserver.mbi.ucla.edu/SAVES) analysis was performed in order to assess the stereo-chemical properties of the three-dimensional models, and Ramachandran plots were calculated. The model with the best Goodness-score of PROCHECK and with the best VERIFY3D profile was subjected to energy minimization using the Discover Module of INSIGHT-II. The binding site was identified using the Pocket finder

program (http://www.modelling.leeds.ac.uk/pocketfinder/). Secondary structure of modeled OXA-51 was assigned using PDBSUM software.

Docking

The chemical structures of penicillinG, ceftazidime, aztreonam, oxacillin, imipenem and nitrocefin were retrieved from the pubchem database (http://pubchem.ncbi.nlm.nih.gov) in two-dimensional MDL/SDF format, and three dimensional coordinates were generated using the CORINA program.

Docking using GLIDE: Grid based Ligand Docking using Energetics

The interaction study of OXA-51 with β-lactam was done using Glide v8 software from Schrodinger (Portland, OR) (http://www.schrodinger.com, 2008). Glide v8 was used for ligand docking in flexible mode as per our earlier protocol [26]. β-lactams were prepared using the "LIGPREP" module. At least one low energy ring conformation was allowed to generate per β-lactam. β-lactam structures were minimized using the 'premin' option with the OPLS_2005 (optimized potential for ligand) force field. OXA-51 was prepared using the protein preparation wizard. The active site of OXA-51 was specified as the centroid of the selected residue in order to generate a grid cube that covered the entire active site. The minimized structures of β-lactams (in SDF) and OXA-51 were used subsequently in docking simulation in HTVS mode, then SP mode followed by XP mode. A flexible Monte-Carlo sampling and minimization were used to identify the best ligand poses for scoring. Five poses were calculated per ligand molecule and docked to the active site of OXA-51. The resulting docked conformations were analyzed using the Glide pose viewer tool. The conformation/pose that made the maximum number of interactions was considered for further analysis.

Docking using GOLD: Genetic optimization for ligand docking

Genetic optimization for ligand docking (GOLD) version 4.1.1 (Cambridge Crystallographic Data Center, Cambridge, UK) was used for docking the molecules in 50 runs using the standard default settings. GOLD v4.1.1 [27] is an automated ligand-docking program that uses a genetic algorithm to explore the full range of ligand conformational flexibility, namely full acyclic ligand flexibility and partial cyclic ligand flexibility, with partial flexibility of the protein in the neighbourhood of the protein active site, and satisfies the fundamental requirement that the ligand must displace loosely bound water on binding. Standard default settings, consisting of population size 100, number of islands 5, selection pressure

1.1, niche size 2, migrate 10, cross over 95, number of operations 1,00,000, number of dockings 50, were adopted for GOLD docking. For ligand-protein binding, 10 docking conformations (poses) were tested and the best GOLD score was selected for studies. In this experiment, 50 genetic algorithms (10 poses in standard) with standard default parameter settings were performed without early termination, after which the 10 best solutions were kept for each ligand. To estimate the protein–ligand complexes, the scoring function GOLD fitness was employed.

Validation of docking results

The binding affinity between the OXA-51 and β-lactams was estimated using the consensus scoring function X-Score V2.1. The two docking algorithms used in the study have different scoring methodologies and therefore it is difficult to compare their scores. To circumvent this problem, the XScore v2.1 [28] scoring function was used. X-Score calculates the negative logarithm of the dissociation constant of the ligand to the protein, $-\log (K_d)$, as the average of three scoring functions (HPScore, HMScore and HSScore), and predicts the binding energy (kcal mol^{-1}) of the ligand. LIGPLOT v4.4 plots the interactions between the GLIDE docked OXA-51 and β-lactam to identify the key interacting atoms [29]. Also, two output files are written where the hydrogen bonded interactions and non-hydrogen bonded interactions are tabulated.

Molecular dynamics simulation

The GLIDE docked complexes were used as the starting structure for MD simulation. The calculations were performed with GROMACS 4.5.3 package [30, 31] using the GROMOS 96 force field. The box dimensions ensured that any protein atom was at least 1.5 Å away from the wall of the box with periodic boundary conditions and solvated by simple point charge (spc) water molecules. The GROMACS topology file for β-lactams was generated using the PRODRG2 server. Cl$^-$ counterions were added to satisfy the electroneutrality condition. Energy minimization was carried out using the steepest descent method. Berendsen temperature coupling and Parrinello-Rahman pressure coupling were used to keep the system in a stable environment (300 k, 1 bar), and the coupling constants were set to 0.1 ps and 2.0 for temperature and pressure, respectively. The partial mesh Ewald (PME) algorithm was employed for electrostatic and Van der Waals interactions; cut-off distance for the short-range VdW (rvdw) was set to 1.4 nm, where Coulomb cut-off (r coulomb) and neighbour list (rlist) were fixed at 0.9 nm. All the bond lengths were constrained using the LINCS algorithm, and the time step was set to 0.002 ps. The complexes in a medium were equilibrated for 100 ps in NPT and NVT ensembles, respectively. Finally, a 5-ns molecular dynamics simulation was carried out for both complexes. All trajectories were stored every 2 ps for further analysis.

Determination of minimal inhibitory concentration

The minimal inhibitory concentration (MIC) of ATCC and resistant clinical strains for ceftazidime, oxacillin, peniciilin, aztreonam and imipenem were determined by the agar dilution method according to our previously described method [22].

Transmission electron microscopy

A. baumannii was examined by transmission electron microscopy (TEM) under different experimental conditions. A resistant strain of *A. baumannii* was cultured in 300 ml LB broth for 12 h at 37°C. The culture was divided into three equal (100 ml each) portions. The first 'control' was without β-lactam, and the second and third portions (100 ml each) contained penicillin (3.2 mg) and imipenem (3.2 mg), respectively. After addition of β-lactam, the cultures were incubated for 7.4 h at 37°C with constant shaking. After the complete time period of 19.4 h growth, the cultures were centrifuged at 7,000 rpm for 15 min. The pelleted cells were washed with PBS buffer (100 mM, pH 7.4) repeatedly. The cells were then fixed with 2.5% glutaraldehyde for 2.5 h at 4°C, after which the cells were washed in fresh PBS buffer. The cells were post-fixed for 2 h in 1% osmium tetroxide in the same buffer at 4°C. After several washes in 100 mM PBS buffer, the cells were dehydrated in graded acetone solutions and embedded in CY 212 Araldite. Ultrathin sections of 60–80 nm thickness were cut using an ultracut E Ultramicrotome and the sections were stained in alcoholic uranyl acetate (10 min) and lead citrate (10 min) before examining the grids in a Philips CM 10 transmission electron microscope operated at 60–80kv. The sections were photographed at 6, 400× magnification. All procedures after the step of fixation were completed in the TEM section of the Sophisticated Analytical Instrumentation Facility (DST), Department of Anatomy, AIIMS.

Results and discussion

In recent years, the number of isolates of *A. baumannii* showing resistance to β-lactams has increased worldwide [32, 33]. β-lactam-resistance due to the presence of OXA β-lactamase has been reported in all over the world [18, 32, our unpublished result]. We found OXA-51 in clinical isolates of *A. baumannii* in our hospital, hence we selected OXA-51 for interaction studies with β-lactams.

Modeling of OXA-51 β-lactamase

As the 3D structure of OXA-51 (274aa) of *A. baumannii* is not available in the data bank, we used homologous modeling in order to generate a 3D model of the protein of interest. A BLASTp search against PDB sequences was performed and results with maximum identity (high score and lower e-value range of 5e-95 to 9e-96) were considered. The results identified β-lactamase in *A. baumannii* identified, 2JC7A (Carbapenemase OXA-24, 244aa), 3FV7A (OXA-24 β-lactamase, 244aa), 3PAEA (K84d Mutant of OXA-2440, 245aa) and 3PAGA (V130d Mutant of OXA-2440, 245aa) as potential templates for building 3D structure of OXA-51 (aa 27–272).

The sequence identity and similarity between target and templates was found to be 67% and 80%, respectively. Amino acid sequence and secondary structural elements of OXA-51 are shown in Fig. 1. Modeled OXA-51 was found to contain 41% α-helix and 18% β-sheet. To validate the homology modeled OXA-51 structure, a PROCHECK Ramachandran Plot was drawn; further analysis revealed the presence of 93% of residues in the core region, with 6.5% in the allowed region and only 0.5% of residues in the disallowed regions (Fig. 2). The Goodness factor (G-factor, obtained from PROCHECK) is essentially a log-odds score based on the observed distribution of stereochemical parameters like quality of covalent and overall bond/angle distances. The G-factors obtained for modeled OXA-51 were −0.37 for dihedrals, −1.45 for covalent bonds, and −0.79 overall, which are within the acceptable range. The energetic architecture as predicted by PROSA score was negative (−8.45) for the modeled protein OXA-51 β-lactamase, which was similar to that obtained for the templates. This indicates the reliability of
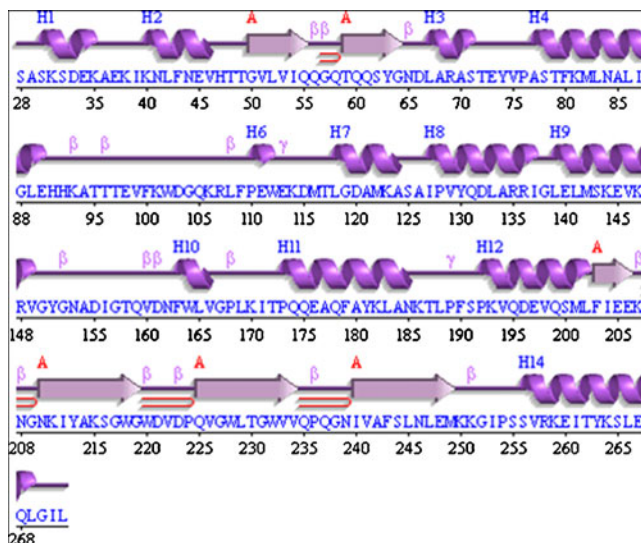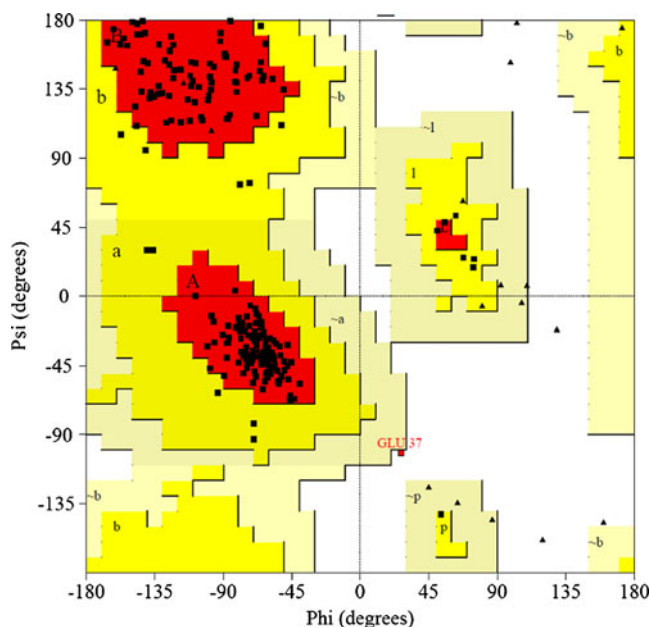

Fig. 2 Ramachandran plot for OXA-51 β-lactamase. The plot shows 93% of amino acid residues of model structure found in the favorable region, suggesting the high quality of the model

Fig. 1 Amino acid sequence of OXA-51 (27–272). The secondary structural elements, α-helix (H1–H14), β-sheet (A), β-turn (β), γ-turn (γ) and β-hairpin (ββ) in the corresponding regions of the sequence are indicated

the model used in the present study. The assessment with VERIFY3D, which derives a "3D-1D" profile based on the local environment of each residue, described by the statistical preferences for the area of the residue that is buried, the fraction of side-chain area that is covered by polar atoms (oxygen and nitrogen) and the local secondary structure, also substantiated the reliability of the 3D structure. The structural superimposition of Cα trace of the OXA-51 model over template structures resulted in a root mean square deviation (RMSD) of 0.3 Å, 67.9% identity, length of alignment for 2JC7_A(0.3 Å, 67.9, 243aa), 3FV7_A (0.3 Å, 67.5, 243aa), 3PAE_A(0.3 Å, 67.5, 243aa) and 3PAG_A(0.3 Å, 67.9, 243aa), respectively, which indicates a valid structure of the model.

The binding site was identified using the pocket finder program on OXA-51 β-lactamase. Amino acid residues involved in the active site of OXA-51 are: Pro76, Ala77, Ser78, Thr79, Lys81, Leu108, Phe109, Glu111, Trp112, Lys 123, Ala124, Ser 125, Ile 127, Gln131, Asn162, Trp164, Leu165, Lys215, Ser216, Gly217, Trp218, Gly219, Trp220, Trp 228, Ser 255 and Arg258 (Fig. 3). Active site residues were used to dock the β-lactams to study their interaction with OXA-51 β-lactamase.

Various β-lactams and their structures

The simplest and oldest penicillin group of antibiotics has the basic structure of 6-amino penicillanic acid (6-APA), which consists of a thiazolidine ring and a β-lactam ring with a variable side chain (R). The side chain R is phenyl-
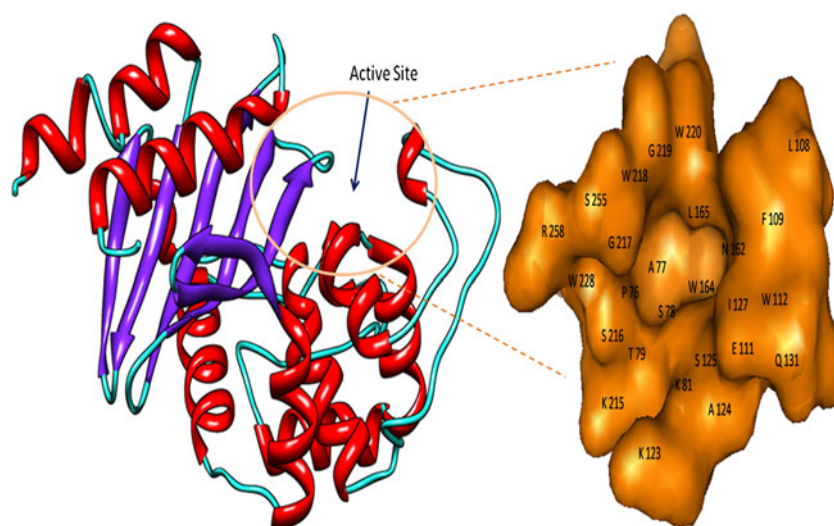
Fig. 3 Three dimensional (3D) structure of OXA-51 from *Acinetobacter baumannii*. *Red* α-Helix, *blue* β-sheet, *cyan* random coil. The magnified region of the active site is shown to the *right*

acetyl in penicillin G and 5-methyl-3-phenyl-oxazole-4-carbonyl in the case of oxacillin. The penicillin nucleus (6-APA) is the chief structural requirement for biological activity and requires the presence of an acid residue on the thiazolidine ring for binding to penicillin-binding proteins (PBPs) [34]. The second group, cephalosporins, which includes ceftazidime, has a β-lactam ring fused to a dihydrothiazine ring [35], while azteronam, which belongs to monobactam group, consists of a naked β-lactam ring with aromatic side chains. The latest generation of β-lactams, carbapenems, including imipenem, resemble penicillins except that the five-membered ring contains a double bond between carbons 2 and 3 and the sulfur atom is replaced by a carbon. As compared to many β-lactam antibiotics, carbapenems are very stable to most β-lactamases. The stability of carbapenems depends on the presence of a simple trans-6-hydroxyethyl group. Analogues with acyl substituents or with 6-hydroxyethyl in the cis configuration are less stable to β-lactamases [34]. The chemical structures of all the lactams used in the present study are shown in Table 1. We also considered nitrocefin, a positive control for β-lactams. Nitrocefin is a homolog of β-lactam and consist of cephan ring. Nitrocefin, yellow in color, is not an antibiotic but has been used in in vitro studies because of its color change to pink upon cleavage by β-lactamase. β-Lactam structures were prepared using the 'LIGPREP' module of Schrodinger software.

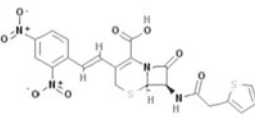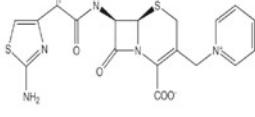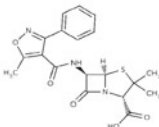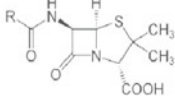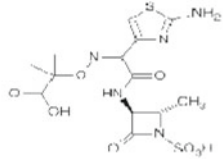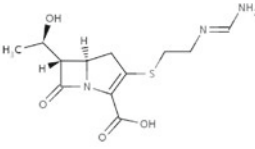Docking of β-lactams with OXA-51

Interaction with nitrocefin

Nitrocefin was used as a positive control as it interacts with β-lactamases. The following 8 hydrogen bonds were observed between nitrocefin and OXA-51 (Fig. 4a) (1) Polar residues: NZ atom of Lys259 of active site forms a hydrogen bond with O8 and O7 of nitrocefin. OE2 atom of Glu111 forms a hydrogen bond with N3 atom of the lactam ring of nitrocefin. OG of Ser 216 and Ser 78 residues form hydrogen bonds with O7 and O5 atoms of nitrocefin, respectively. Similarly, NH2 and NH1 of Arg258 in the active site form hydrogen bonds with O6 of nitrocefin. (2) Nonpolar residues: NE1 atom of Trp 112 hydrogen bonds with O2 atom of the nitrocefin (Table 1). Ligplot of nitrocefin and protein suggested that it forms 8 hydrogen bonds and 12 non-hydrogen bonds (Table 2). As noted in Materials and methods, the GLIDE score represents docking energy, and therefore a low GLIDE score indicates strong binding. The OXA51–nitrocefin interaction gave a GLIDE score of −9.95 kcal mol^{-1}. The X-score function includes terms for van der Waals interaction, hydrogen bonding, deformation penalty and hydrophobic effects. X-Score performs better in identifying the correct bound conformations used for docking analysis. Glide docked OXA51-nitrocefin structure gave an X-score of −7.61 kcal mol^{-1}. GOLD fitness of this complex also has good value (58.16) and is among the top rankers.

Interaction with ceftazidime

Ceftazidime was observed to interact with OXA-51 by forming eight hydrogen bonds (Fig. 4b) involving Lys 259, Ser 255, Ser 216, Lys 213 and Glu 111. Ceftazidime forms most hydrogen bonds as compared to other β-lactams. NZ of Lys259 is hydrogen bonded with O7 and O6 of ceftazidime. OG atom of Ser 255 and Ser 216 forms a hydrogen bond with the O6 atom of ceftazidime. The O atom of Lys123 interacts with the N1 atom of ceftazidime via hydrogen bonding. OE2 atom of Glu111 forms a hydrogen bond with N3 of ceftazidime, and the OE1 atom of

Table 1 Hydrogen bond interactions between β-lactam and OXA-51 using X-Score from GLIDE

β-lactam	A.A residues in OXA-51	Interacting atoms		
		OXA-51	β-lactam	Distance (Å)
Nitrocefin (Positive control)	LYS 259	NZ	O8	3.32
	LYS 259	NZ	O7	2.65
	ARG 258	NH2	O6	2.93
	ARG 258	NH1	O6	3.24
	SER 216	OG	O7	2.89
	TRP 112	NE1	O2	3.00
	GLU 111	OE2	N3	2.64
	SER 78	OG	O5	3.14
Ceftazidime	LYS 259	NZ	O7	3.00
	LYS 259	NZ	O6	3.09
	SER 255	OG	O6	2.91
	SER 216	OG	O6	2.80
	LYS 123	O	N1	2.92
	GLU 111	OE2	N3	2.94
	GLU 111	OE1	N6	2.90
	GLU 111	OE1	N5	2.76
Oxacillin	LYS 259	NZ	O3	2.92
	LYS 259	NZ	O2	2.85
	SER 125	OG	O1	3.09
	GLU 111	OE2	N3	2.47
Penicillin	LYS 259	NZ	O4	2.76
	SER 125	OG	O1	2.96
	GLU 111	OE2	N2	2.92
Aztreonam	LYS 259	NZ	O7	2.66
	LYS 123	NZ	O8	2.71
	LYS 123	NZ	O7	3.02
	GLU 111	OE2	N1	3.03
	GLU 111	OE1	N5	2.77
Imipenem	ARG 258	NH2	O4	3.16
	ARG 258	NH2	O3	3.01
	SER 125	OG	O2	2.95
	GLU 111	OE2	N2	2.68
	GLU 111	OE1	N3	2.76

Glu111 interacts with the N6 and N5 atoms of Ceftazidime (Table 1). The GLIDE score for ceftazidime-OXA51 docking was found to be −8.78 kcal mol^{-1} and the X-score of the Glide docked complex was −7.50 kcal mol^{-1} (Table 2).

Ceftazidime had the highest GOLD fitness score (65.38). All the results conclude unequivocally that ceftazidime interacts strongly with OXA-51 and therefore is cleaved efficiently by OXA-51.
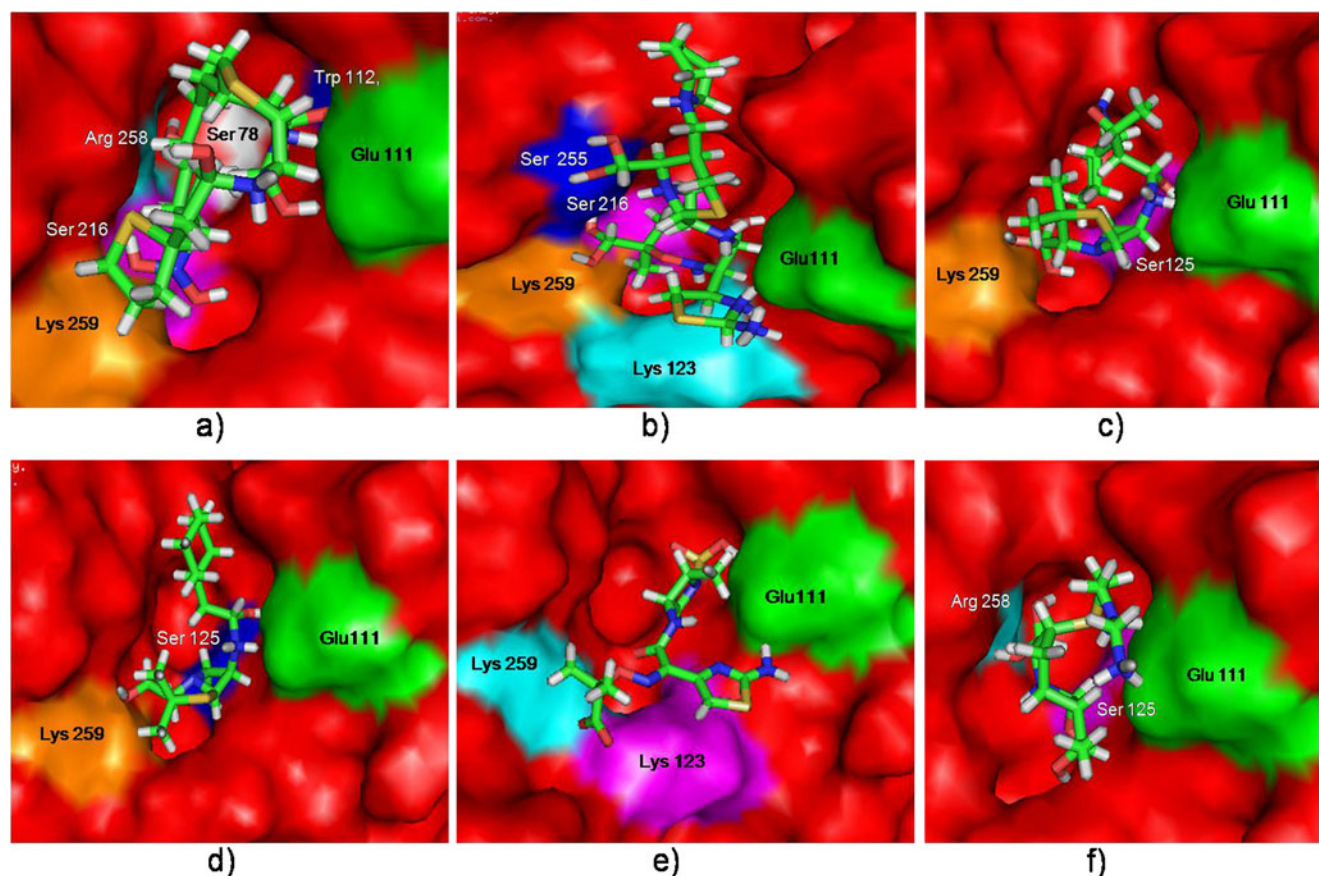
Fig. 4 Docked complexes of β-lactam in the active site of OXA-51 of *A. baumannii*. **a** Nitrocefin, **b** ceftazidime, **c** oxacillin, **d** penicillin, **e** aztreonam, **f** imipenem. OXA-51 is depicted in surface view and β-lactams in stick view

Interaction with oxacillin

Four hydrogen bond interactions, involving residues Lys 259, Ser 125 and Glu 111, were observed between oxacillin and OXA-51 (Fig. 4c, Table 1). GLIDE score for docking of oxacillin with OXA-51 was −8.45 kcal mol^{-1} and its corresponding X-score was −7.83 kcal mol^{-1}. The GOLD X-score of oxaciliin-OXA51 docking was −7.01 kcal mol^{-1}. GLIDE and GOLD X-scores were found to be lowest for

oxacillin (Table 2), which confirms that oxacillin interacts with OXA-51 with high affinity. This high binding affinity comes from its 19 non-hydrogen bond interactions that are present between oxacillin and OXA-51 (Table 2).

Interaction with penicillin

OXA-51 formed three hydrogen bonds with penicillin using Lys 259, Ser 125 and Glu 111 (Fig. 4d, Table 1). The GLIDE score

Table 2 Interaction parameters of various β-lactams with OXA-51 using the software GLIDE and GOLD. Number of hydrogen bonds and non-hydrogen bonds were derived from LIGPLOT

β-Lactam	GLIDE		GOLD		Number of hydrogen bonds	Number of non-hydrogen bonds
	Score (kcal/mol)	X-score (kcal/mol)	Fitness	X-score (kcal/mol)		
Nitrocefin	−9.95	−7.61	58.16	−6.35	8	12
Ceftazidime	−8.78	−7.50	65.38	−6.05	8	11
Oxacillin	−8.45	−7.83	45.70	−7.01	4	19
Penicillin	−7.88	−7.09	50.29	−6.96	3	7
Aztreonam	−8.60	−6.80	52.27	−5.93	5	6
Imipenem	−7.12	−6.19	47.94	−5.26	5	9

for docking of penicillin with OXA51 was −7.88 kcal mol^{-1} and the corresponding X-score was −7.09 kcal mol^{-1}. The GLIDE X-score of this complex was found to be higher than that of ceftazidime and oxacillin. The GOLD X-score for this docking was −6.96 kcal mol^{-1} and was found to be higher only than oxacillin (−7.01 kcal mol^{-1}) (Table 2). The X-score results clearly showed that penicillin has a high affinity with OXA-51; its affinity is comparable to that of oxacillin and ceftazidime, which have highest affinity. Because penicillin forms fewer hydrogen bonds compared with ceftazidime, aztreonam and oxacillin, it is less directional than these β-lactams.

Interaction with aztreonam

The aztreonam–OXA-51 complex is stabilized by five hydrogen bonds. Lys 259, Lys 123 and Glu 111 of OXA-51 are involved in hydrogen bonding with aztreonam (Fig. 4e, Table 1). The GLIDE score for docking of aztreonam in the active site of OXA-51 was −8.60 kcal mol^{-1} and its corresponding X-score was −6.80 kcal mol^{-1}. The GLIDE X-score was found to be higher than that of any other β-lactam except carbapenem (imipenem). The GOLD X-score of this interaction was −5.93 kcal mol^{-1}, which was found to be higher than all the interacting β-lactams except imipenem (Table 2). These results reveal that aztreonam (monobactam) has low binding affinity compared to other β-lactams except carbapenem, which has an even lower binding affinity.

Interaction with imipenem

Imipenem is a well known antibiotic belonging to the carbapenem group of antibiotics. It was observed that imipenem interacts with OXA-51 by forming five hydrogen bonds (Fig. 4f, Table 1). It can be seen that ceftazidime, which strongly binds to OXA-51, makes the highest number of hydrogen bonds (eight). The NH2 of Arg 258 of OXA-51 forms two hydrogen bonds with O3 and O4 atom of imipenem. OG of Ser 125 in the active site forms a hydrogen bond with the O2 atom of imipenem. OE1 and OE2 atoms of Glu111 of the active site form hydrogen bonds with N2 and N3 atoms of imipenem. Two hydrogen bonds in the imipenem–OXA-51 complex are weak (>3 Å). The molecular distance between the OE2 atom of Glu111 and N1 atom of β-lactam ring of imipenem was found to be highest (6 Å) of all the β-lactams studied here. Lys 259 of OXA-51 participated in hydrogen bond formation with all β-lactams studied, i.e., ceftazidime, oxacillin, penicillin and aztreonam, but surprisingly does not make any contacts with imipenem. This is an important and interesting finding that points to the fact that Lys 259 is vital in the enzyme activity of OXA-51 in cleaving the β-lactam ring. The GLIDE score for imipenem and OXA-51 docking was −7.12 kcal mol^{-1}

and its corresponding X-score was −6.19 kcal mol^{-1} (Table 2). GOLD fitness for this docking was 47.94 and its corresponding X-score was −5.26 kcal mol^{-1}. It was also observed that imipenem had highest value of GLIDE and GOLD X-scores (−6.19 and −5.26 kcal mol^{-1}), which means that it has weakest affinity with OXA-51 (Table 2). Due to the low affinity of imipenem it may not be cleaved efficiently by OXA-51. Hence it can be concluded that the newly discovered carbapenem (imipenem) group of β-lactams antibiotics show only a weak interaction with OXA-51 and are not readily cleaved by it. Based on the present results, the order of interaction of β-lactams with OXA-51 was found to be: ceftazidime > oxacillin > penicillin > aztreonam > imipenem.

Molecular dynamics simulations

To explore the stabilities and dynamic characteristics of OXA-51 complexed with imipenem and ceftazidime, we carried out MD simulations based on GLIDE docking conformations. These two β-lactam-OXA-51 complexes were selected because imipenem has least binding and ceftazidime has maximum binding with OXA-51. The RMSDs of β-lactams relative to OXA-51, and OXA-51 relative to its original conformation were calculated (Fig. 5) and indicate that both systems reached equilibrium within the simulation time and that the enzyme was stable throughout the simulation at a RMSD value of 2.5 Å, but the RMSDs of β-lactams are quite different.

Figure 5a shows the RMSD of ceftazidime relative to OXA-51. This system approaches equilibrium at 3 ns and is stable throughout the MD simulation, suggesting a stable binding of ceftazidime with OXA-51. Figure 5b shows that the RMSD of imipenem relative to OXA-51 increases within the first 2.5 ns and then the complex becomes partially stable throughout the simulation. Interactions between imipenem and OXA-51 are weak throughout the simulation but remain at the binding pocket. MD simulation studies show that β-lactams can bind steadily to OXA-51. Hydrogen bonding analysis revealed that imipenem shares 1–2 hydrogen bonds while ceftazidime showed 3–5 hydrogen bonds with OXA-51 throughout the simulation. The average structure of the MD simulation also showed more interaction of OXA-51 to ceftazidime as compared to imipenem. This clearly suggests that imipenem is associated only weakly with OXA-51 and may not be cleaved by OXA-51. MD results are in full agreement with the docking results. Interestingly, a Ligplot of the MD-simulated complexes of β-lactams with OXA-51 clearly indicates the importance of Glu111, which participated in the interaction throughout simulation.

Bioinformatic results were further validated by experimental findings of MIC and TEM. The wild type or ATCC of *A. baumannii* is sensitive to all β-lactams, irrespective of the
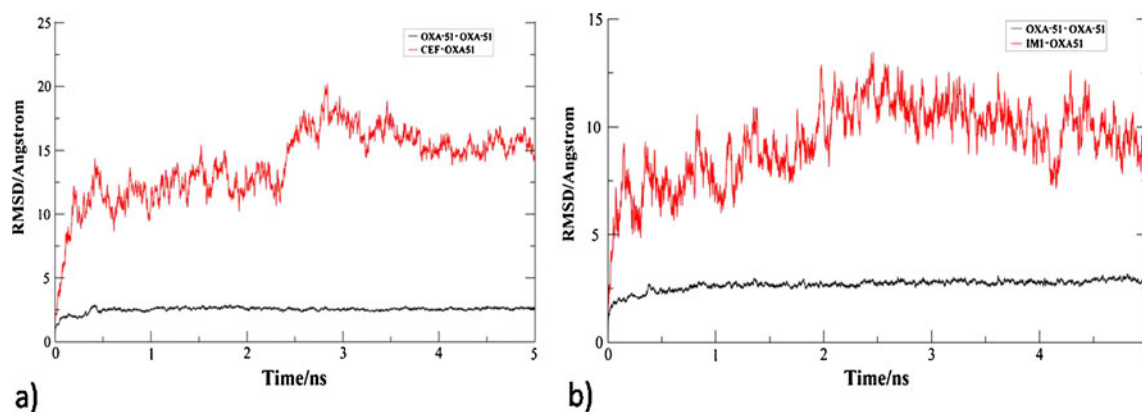
Fig. 5 Time dependence of root mean square deviations (RMSDs) from molecular dynamics (MD) simulations of **a** ceftazidime–OXA-51 complex and **b** imipenem–OXA-51 complex

type of group. The MIC was always <1 μg ml^{-1}; however, the resistant *A. baumannii* reacted differently depending on the type of β-lactam. It should be noted that OXA-51 is produced only by *A. baumannii* under resistant conditions and not in wild type (ATCC). Thus, comparing the MIC of different antibiotics shows how the organism responds to a given type of β-lactam. The low MIC means that *A. baumannii* is killed easily and high MIC means the bacterium is more difficult to kill. The MIC data of the four groups of antibiotics was follows: cephalosporin group-256 μg ml^{-1} (for ceftazidime), penicillin group-128 μg ml^{-1} and monobactam group-128 μg ml^{-1} (for aztreonam) and carbapenem group-64 μg ml^{-1} (for imipenem). It is therefore evident that the carbapenem group has the lowest MIC compared to other β-lactams, hence a lower concentration of imipenem is required to kill *A. baumannii*. Low MIC values of imipenem were also reported in *Pseudomonas aeruginosa* harboring OXA-2 β-lactamase [36]. Therefore, docking results correlate well with MIC data. The high MIC observed with ceftazidime clearly suggests the inefficiency of ceftazidime against resistant *A. baumannii*.

In the absence of β-lactams (control), *A. baumannii* shows its natural morphology of a coccobacillus structure, and an intact membrane structure can be seen in TEM images (Fig. 6, left panel). In the presence of imipenem, the results were drastic, as the shape of the bacterium changed completely, and rapid cell lysis occurred with the release of the cell contents, leaving a 'spheroplast'. The cells were completely empty as the cytoplasm had diffused out of the cell membranes due to increased porosity of the membranes (Fig. 6, right panel). This suggests that imipenem kills the bacteria. However, in the presence of penicillin, the cell membrane did not change drastically; the cells were osmotically stable and remained as spherical shaped cells (Fig. 6, center). Hence bioinformatic results show good correlation with the cell morphological changes as seen in TEM, which also support the potency of imipenem. Although drug resistance is a multifactorial phenomenon, the weak interaction of OXA-51 with the carbapenem might be a factor responsible for its low MIC. Hence we can say that OXA-51 plays a very significant role in the resistance of *A. baumannii*.
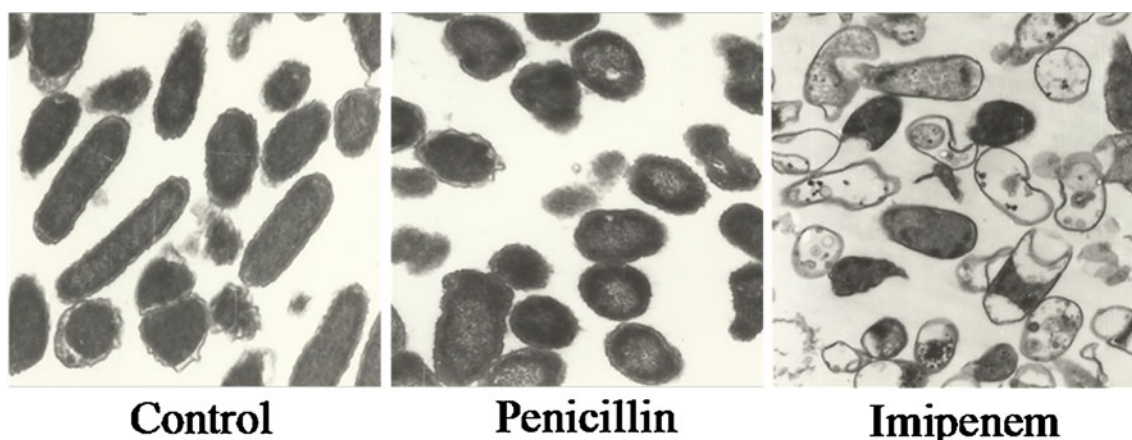

Fig. 6 Transmission electron microscopy (TEM) of a resistant strain of *A. baumannii* under antibiotic stress at 6,400 × magnification. *Left A. baumannii* without antibiotics (control), *center* + 64 μg ml^{-1} penicillin, *right* + 64 μg ml^{-1} imipenem

Conclusions

The present study provides a relationship between efficiency of binding of β-lactams to OXA-51 and the observed resistance in *A. baumannii*. The results provide strong evidence of the involvement of residue Glu111 of OXA-51 in binding to β-lactams. OXA-51 showed strong binding affinity with the cephalosporin and penicillin groups of β-lactams, suggesting the high efficiency of OXA-51 in cleaving these antibiotics. On the contrary, the lowest affinity of carbapenem to OXA-51 clearly indicates the low enzyme activity of OXA-51, which in turn correlates well with the fact that carbapenem is still the most effective β-lactam. Further experimental MIC and TEM data strongly support the conclusions drawn based on bioinformatics. These findings help to understand the role of OXA-51 in resistance and will further help in the development of more efficient β-lactam-based drugs against resistant strains of *A. baumannii*.

References

1. Gaynes R, Edwards JR (2005) Overview of nosocomial infections caused by gram-negative bacilli. Clin Infect Dis 41:848–854. doi:10.1086/432803
2. Davis KA, Moran KA, McAllister CK, Gray PJ (2005) Multidrug-resistant *Acinetobacter* extremity infections in soldiers. Emerg Infect Dis 11:1218–1224
3. Jones RN, Sader HS, Fritsche TR (2005) Comparative activity of doripenem and three other carbapenems tested against Gram-negative bacilli with various β-lactamase resistance mechanisms. Diagn Microbiol Infectious Dis 52:71–74. doi:10.1016/j.diagmicrobio.2004.12.008
4. Scott P, Deye G, Srinivasan A, Murray C, Moran K, Hulten E et al (2007) An outbreak of multidrug-resistant *Acinetobacter baumannii-calcoaceticus* complex infection in the US military health care system associated with military operations in Iraq. Clin Infect Dis 44:1577–1584. doi:10.1086/518170
5. Hawley JS, Murray CK, Griffith ME, McElmeel ML, Fulcher LC, Hospenthal DR et al (2007) Susceptibility of *Acinetobacter* strains isolated from deployed US military personnel. Antimicrob Agents Chemother 51:376–378. doi:10.1128/AAC.00858-06
6. Griffith ME, Lazarus DR, Mann PB, Boger JA, Hospenthal DR, Murray CK (2007) *Acinetobacter* skin carriage among US army soldiers deployed in Iraq. Infect Control Hosp Epidemiol 28:720–722. doi:10.1086/518966
7. Neonakis IK, Spandidos DA, Petinaki E (2011) Confronting multidrug-resistant *Acinetobacter baumannii*: a review. Int J Antimicrob Agents 37:102–109. doi:10.1016/j.ijantimicag.2010.10.014
8. Ho PL, Cheng VC, Chu CM (2009) Antibiotic resistance in community-acquired pneumonia caused by *Streptococcus pneumoniae*, methicillin-resistant *Staphylococcus aureus*, and *Acinetobacter baumannii*. Chest 136:1119–1127. doi:10.1378/chest.09-0285
9. Villegas MV, Hartstein AI (2003) *Acinetobacter* outbreaks, 1977–2000. Infect Control Hosp Epidemiol 24:284–295. doi:10.1086/502205
10. Maragakis LL, Cosgrove SE, Song X, Kim D, Rosenbaum P, Ciesla N et al (2004) An outbreak of multidrug-resistant *Acinetobacter baumannii* associated with pulsatile lavage wound treatment. JAMA 292:3006–3011. doi:10.1001/jama.292.24.3006
11. Maragakis LL, Perl TM (2008) *Acinetobacter baumannii*:epidemiology, antimicrobial resistance, and treatment options. Clin Infect Dis 46:1254–1263. doi:10.1086/529198
12. Paterson DL (2006) The epidemiological profile of infections with multidrug-resistant *Pseudomonas aeruginosa* and *Acinetobacter* species. Clin Infect Dis 43:S43–S48. doi:10.1086/504476
13. Fournier PE, Richet H, Weinstein RA (2006) The epidemiology and control of *Acinetobacter baumannii* in health care facilities. Clin Infect Dis 42:692–699. doi:10.1086/500202
14. Gupta E, Mohanty S, Sood S, Dhawan B, Das BK, Kapil A (2006) Emerging resistance to carbapenems in a tertiary care hospital in north India. Indian J Med Res 124:95–98
15. Zavascki AP, Carvalhaes CG, Picao RC, Gales AC (2010) Multidrug-resistant *Pseudomonas aeruginosa* and *Acinetobacter baumannii*:resistance mechanisms and implications for therapy. Expert Rev Anti Infect Ther 8:71–93. doi:10.1586/eri.09.108
16. Doi Y, Husain S, Potoski BA, McCurry KR, Paterson DL (2009) Extensively drug resistant *Acinetobacter baumannii*. Emerg Infect Dis 15:980–982. doi:10.3201/eid1506.081006
17. Vila J, Pachon J (2008) Therapeutic options for *Acinetobacter baumannii* infections. Expert Opin Pharmacother 9:587–599. doi:10.1517/14656566.9.4.587
18. Hu WS, Yao S, Hsieh CF, Liu C, Lin J (2007) An OXA-66/OXA-51-Like Carbapenemase and Possibly an Efflux Pump Are Associated with Resistance to Imipenem in *Acinetobacter baumannii*. Antimicrob Agents Chemother 51:3844–3852. doi:10.1128/AAC.01512-06
19. Acosta J, Merino M, Viedma E, Poza M, Sanz F, Otero JR et al (2011) Multidrug-resistant *Acinetobacter baumannii* harboring OXA-24 carbapenemase, spain. Emerg Infect Dis 17:6. doi:10.3201/eid1706.091866
20. Brown S, Amyes S (2006) OXA β-lactamases in Acinetobacter: the story so far. J Antimicrob Chemother 57:1–3. doi:10.1093/jac/dki425
21. Vashist J, Rajeswari MR (2006) Structural investigations on a novel porin, OmpAb from *Acinetobacter baumannii*. J Biomol Struct Dyn 24:243–253
22. Vashist J, Tiwari V, Das R, Kapil A, Rajeswari MR (2011) Analysis of penicillin-binding proteins (PBPs) in carbapenem resistant *Acinetobacter baumannii*. Indian J Med Res 133:332–338
23. Vashist J, Tiwari V, Kapil A, Rajeswari MR (2010) Quantitative profiling and identification of outer membrane proteins of β-Lactam resistant strain of *Acinetobacter baumannii*. J Proteome Res 9:1121–1128. doi:10.1021/pr9011188
24. Culebras E, González-Romo F, Head J, Gómez M, Morales G, Picazo JJ (2010) Outbreak of *Acinetobacter baumannii* producing OXA-66 in a Spanish hospital: epidemiology and study of patient movements. Microb Drug Resist 16:309–315. doi:10.1089/mdr.2009.0113
25. Papa A, Koulourida V, Souliou E (2009) Molecular epidemiology of carbapenem-resistant *Acinetobacter baumannii* in a newly established greek hospital. Microbial drug resistance 15:257–260. doi:10.1089/mdr.2009.0060
26. Vashist J, Vishvanath, Kapoor R, Kapil A, Yennamalli R, Subbarao N, Rajeswari MR (2009) Interaction of nalidixic acid and ciprofloxacin with wild type and mutated quinolone-resistance-determining region of DNA gyrase A. Indian J Biochem Biophys 46:147–153
27. Rarey M, Kramer B, Lengauer T, Klebe G (1996) A fast flexible docking method using an incremental construction algorithm. J Mol Biol 261:470–489. doi:10.1006/jmbi.1996.0477

28. Wang R, Lai L, Wang S (2002) Further development and validation of empirical scoring functions for structure-based binding affinity prediction. J Comput Aided Mol Des 16:11–26. doi:10.1023/A:1016357811882

29. Wallace AC, Laskowski RA, Thornton JM (1995) LIGPLOT:a program to generate schematic diagrams of protein ligand interactions. Protein Eng 8:127–134. doi:10.1093/protein/8.2.127

30. Spoel DVD, Lindahl E, Hess B, Groenhof G, Mark AE, Berendsen HJC (2005) GROMACS:Fast, flexible, and free. J Comput Chem 26:1701–1718. doi:10.1002/jcc.20291

31. Lindahl E, Hess B, Spoel DVD (2001) GROMACS 3.0:a package for molecular simulation andtrajectory analysis. J Mol Model 7:306–317. doi:10.1007/s008940100045

32. Yang HY, Lee HJ, Suh JT, Lee KM (2009) Outbreaks of Imipenem resistant *Acinetobacter baumannii* producing OXA-23 β-Lactamase in a tertiary care hospital in Korea. Yonsei Med J 50:764–770. doi:10.3349/ymj.2009.50.6.764

33. Feizabadi MM, Fatholllahzadeh B, Taherikalani M, Rasoolinejad M, Sadeghifard N, Aligholi M et al (2008) Antimicrobial suscep-tibility patterns and distribution of bla$_{OXA}$ genes among *Acineto-bacter spp.* isolated from patients at Tehran hospital. Jpn J Infect Dis 61:274–8

34. Shahid M, Sobia F, Singh A, Malik A, Khan HM, Jonas D, Hawkey PM (2009) Beta-lactams and Beta-lactamase-inhibitors in current- or potential- clinical practice: a compre-hensive update. Crit Rev Microbiol 35:81–108. doi:10.1080/10408410902733979

35. Yao JD, Moellering RC (1991) Antimicrobial agents. In: Balows A, Houston W, Hermann KL, Isenberg H (eds) Manual of Clinical Microbiology, 5th edn. American Society for Microbiology, Washington, DC, pp 1065–1099

36. Danel F, Hall LMC, Gur D, Livermore DM (1997) OXA-15, an extended-spectrum variant of OXA-2 β-Lactamase, isolated from a *Pseudomonas aeruginosa* strain. Antimicrob Agents Chemother 41:785–790